

Visibility and Connectivity Analysis of LEO Satellite Networks under LoRa Protocols

Junse Lee
School of AI Convergence
Sungshin Women's University
Seoul, Korea
junselee@sungshin.ac.kr

Sooyeob Jeong, Joon Gyu Ryu
Satellite Wide-Area Infra Research Section
Electronics and Telecommunications Research Institute
Daejeon, Korea
jung2816@etri.re.kr, jgryurt@etri.re.kr

Abstract—This paper proposes a new framework for analyzing the LEO satellite networks under the LoRa protocol. By modeling the location of LEO satellites as a Poisson point process on the spherical cap, we characterize the connectivity and visibility of LEO satellites observed by the typical user.

Index Terms—LEO satellites, LoRa

I. INTRODUCTION

The satellite networks are promising network architecture to support global coverage in the beyond 5G and 6G era [1]. Among them, low-Earth-orbit (LEO) satellites have been widely considered due to their low latency and high data rates [2]. In recent years, many applications of the Internet of Things (IoT) using LEO satellite networks have developed in many areas such as agriculture, maritime, military things and so on.

In order to achieve large-scale connectivity and low power consumption, Long Range (LoRa) signal [3] becomes one of the main research directions of IoT satellite networks. So, understanding the LEO satellite networks under the LoRa protocol is important in terms of system parameters to optimize satellite deployment. We use the stochastic geometry to analyze the network performance by spatially averaging the performances of wireless networks. Prior works have been conducted on this mathematical tool to analyze LEO satellite networks [2], but the analysis of LEO satellite networks under the LoRa protocol has not been much studied. In this paper, we propose a new framework to analyze the visibility and connectivity of LEO satellites observed by the typical IoT user on the ground by adopting the stochastic geometry.

II. SYSTEM MODEL

In this section, we present the network model for LEO satellite networks under the LoRa protocol.

A. LoRa Signal

LoRa signal is based on a chirp spread spectrum (CSS) for low power wide area network (LPWAN) applications. This uses a quasi-orthogonal spreading factor (SF) to increase the network performance. LoRa signal contains

TABLE I
LoRa CHARACTERISTIC WHERE $B = 125kHz$.

SF	Bit Rate	Receiver Sensitivity	SNR Threshold
7	5.469kbps	-124.5dBm	-7.5dB
8	3.125kbps	-127dBm	-10dB
9	1.758kbps	-129.5dBm	-12.5dB
10	0.977kbps	-132dBm	-15dB
11	0.537kbps	-134.5dBm	-17.5dB
12	0.293kbps	-137dBm	-20dB

important parameters such as 1) sub-channel bandwidth (B), and 2) SF, which can be set from 7 to 12 under different signal-to-noise ratio (SNR) thresholds. Table I presents the LoRa characteristic, which shows the relation between SF, bit rate, receiver sensitivity, and SNR threshold where $B = 125kHz$.

B. Network Geometry

We assume that the Earth is a perfect sphere with a radius R_E and the altitude of LEO satellites from the ground is R_h . So, all satellites are located on the sphere with a radius $R = R_h + R_E$. Further, we assume that satellites are distributed on this sphere with radius R according to a homogeneous Poisson point process (PPP) with an intensity λ_s . Let us denote the location of satellites by $\{\mathbf{x}\} = \{\mathbf{x}_1, \mathbf{x}_2, \dots, \mathbf{x}_N\}$ where N is a Poisson random variable with mean $4\pi R\lambda$. In this paper, we are interested in a user's visibility and connectivity to the LEO satellite networks. We refer to this user as the typical user. Without loss of generality, we assume that the center of Earth and the typical user are located at $(0, 0, 0)$ and $(0, 0, R_E)$ of the three-dimensional Cartesian coordinate \mathbb{R}^3 , respectively as in the left figure of Fig 1.

The right figure of Fig 1 illustrates the top view of the visibility area observed by the typical user to emphasize the effect of the SF parameter setting. This area is divided into six regions and named as $\mathcal{A}_7, \mathcal{A}_8, \dots, \mathcal{A}_{12}$. We assume that satellites in \mathcal{A}_i with $i = 7, 8, \dots, 12$ communicate with the typical user by LoRa signal with SF = i . In other words, the typical user transmits SF7, and SF12 LoRa signals to communicate with satellites in the

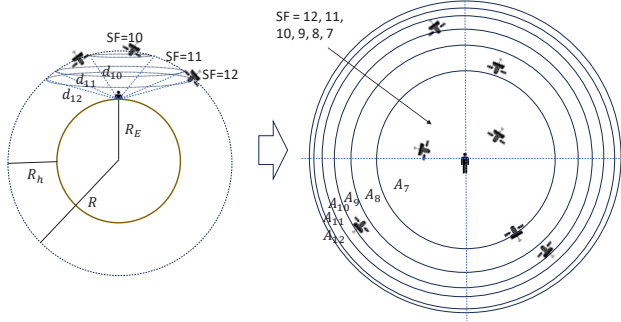


Fig. 1. Illustration of network geometry and top view of LEO satellite from the zenith of the user to illustrate SF parameter.

innermost area and the outermost area, respectively. \mathcal{A}_i is determined by the sensitivity level. So, we introduce d_i for $i = 7, 8, \dots, 12$, which is the maximum distance from the typical user, which supports the minimum sensitivity level of the i -th SF under no fading. For example, d_i under $B = 125kHz$ is

$$d_i = \left(10^{\frac{124.5 + 2.5(i-7)}{10}} GP_t \right)^{\frac{1}{\alpha}} \quad (1)$$

where P_t is the typical user's transmit power, G is the transmit antenna gain, α is the path-loss exponent.

III. CONNECTIVITY AND VISIBILITY

In this section, we provide some results regarding the connectivity and visibility of LEO satellites under the LoRa protocol. For the readability of the following theorems, we assume $d_6 = 0$.

Theorem 1: The number of satellites in \mathcal{A}_i follows a Poisson random variable with mean

$$\lambda_s \pi R \left(\frac{2R_E R + (d_i^2 - d_{i-1}^2) - R^2 - R_E}{R_E} \right), \quad (2)$$

for $i = 7, 8, \dots, 12$.

The next corollary comes from the following Theorem 1.

Corollary 1: The probability that there is no satellite in \mathcal{A}_i is

$$\exp \left(-\lambda_s \pi R \left(\frac{2R_E R + (d_i^2 - d_{i-1}^2) - R^2 - R_E}{R_E} \right) \right), \quad (3)$$

for $i = 7, 8, \dots, 12$.

Theorem 2: Let l_i be the distance between the typical user and its nearest LEO satellite in \mathcal{A}_i . Assuming that if there exists at least one satellite in \mathcal{A}_i , then the distribution of l_i becomes

$$f(l_i) = 2\lambda\pi l_i \frac{R}{R_E} \exp \left(-2\pi\lambda R \left(\frac{\lambda\pi(d_{i-1}^2 - l_i^2)}{R_E} \right) \right) \quad (4)$$

for $d_{i-1} \leq l_i \leq d_i$ where $i = 7, 8, \dots, 12$.

The proof of Theorem 2 is omitted due to the page limitation. The basic principle comes from calculating the derivative of the void probability of PPP.

IV. NUMERICAL EXPERIMENTS

For the numerical analysis, we assume that $R_E = 6371(km)$, $R_h = 500(km)$, $\alpha = 2$, $P_t = 20dBm$, $G = 6dB$, and $\lambda_s = 0.0005$. This leads $d_7 = 1061(km)$, and $d_8 = 1415(km)$, and so on. In this case, Figure 2 illustrates the distribution of l_i . We can simply check that our analytic expressions are well-matched with the simulation results.

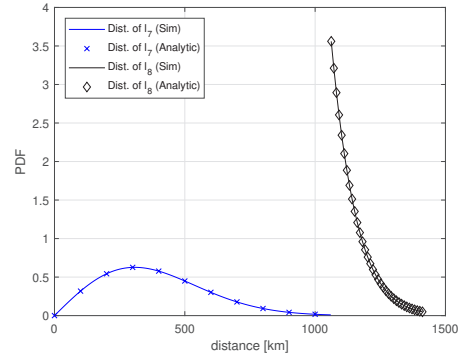


Fig. 2. Distribution of l_7 and l_8 .

V. CONCLUSION

This paper analyzed the visibility and connectivity observed by the typical user under LEO satellite networks. By modeling the location of satellites as a homogeneous PPP on the spherical region, we obtain the distribution of the number of satellites communicating under a specific value of SF with the typical user. We verified that the analytical expressions and the simulation results are well-matched to provide intuitions on how network parameters are affected by the network performances.

ACKNOWLEDGMENT

This work was supported by Institute of Information & communications Technology Planning & Evaluation (IITP) grant funded by the Korea government (MSIT) (No.2020-0-00843, Development of low power satellite multiple access core technology based on LEO cubesat for global IoT service).

REFERENCES

- [1] S. Chen, et al. "Vision, requirements, and technology trend of 6G: How to tackle the challenges of system coverage, capacity, user data-rate and movement speed." *IEEE Wireless Communications* 27.2 (2020): 218-228.
- [2] B. Al Homssi, et al. "Next Generation Mega Satellite Networks for Access Equality: Opportunities, Challenges, and Performance." *IEEE Communications Magazine* 60.4 (2022): 18-24.
- [3] W. Ayoub, et al. "Internet of Mobile Things: Overview of LoRaWan, DASH7, and NB-IoT in LPWANs standards and supported mobility." *IEEE Communications Surveys & Tutorials* 21.2 (2018): 1561-1581.